Using a confined space to boost the driving amplitude of pulsating bubbles to facilitate jetting

Craig Stuart Carlson, Nicole Anderton, Vered Aharonson, Naoyuki Otake, Hu Xinyue, Momoka Yamasaku, Mamoru Hashimoto, Nobuki Kudo, Michiel Postema

Craig S. Carlson*, Nicole Anderton, Vered Aharonson, Naoyuki Otake, Hu Xinyue, Momoka Yamasaku, Mamoru Hashimoto, Nobuki Kudo, and Michiel Postema

Using a confined space to boost the driving amplitude of pulsating bubbles to facilitate jetting

https://doi.org/10.1515/

Abstract: A bubble collapsing near an interface may result in the formation of a liquid jet protruding from the distal bubble side, through the bubble, towards the interface. Ultrasound assisted jetting has been observed when subjecting, by approximation, infinite fluids to acoustic amplitudes above the inertial cavitation threshold, limiting the possibility of ultrasound-guided, bubble-assisted drug or gene delivery. However, the vascular system can be regarded as a finite fluid. The purpose of this study was to investigate the feasibility of low-amplitude jetting for fluid containing biocompatible cavitation nuclei, by placing the region of interest in a confined space to ensure a standing wave field. Droplets of Quantison™ ultrasound contrast agent were pipetted into a Perspex cylindrical compartment of 8-mm diameter and 2-mm height, which was part of an imaging system. The contrast agent was subjected to 3-cycle ultrasound pulses with a centre frequency of 1 MHz whilst being observed at a frame rate of ten million frames per second. Jetting was observed to occur with microbubbles nucleated from the contrast agent in an acoustic regime whose free-field mechanical index was 0.6. Empirical curve matching showed a pulse amplification by a factor of six owing to the chosen geometry. Visible jet lengths of twice the bubble radius on the verge of collapse were measured. Owing to the confined space, the local acoustic amplitude was amplified to surpass the cavitation threshold. This finding is of interest for medical ultrasonic applications where the local environment comprises reflectors.

Keywords: Liquid jets, high-speed photography, ultrasound contrast agent, Quantison™, standing field.

***Corresponding author: Craig S. Carlson,** Department of Electrical Engineering and Automation, Aalto University, Maarintie 8, 02150 Espoo, FI; Department of Biomedical Technology, Faculty of Medicine and Health Technology, Tampere University, Korkeakoulunkatu 3, 33720 Tampere, FI and School of Electrical and Information Engineering, University of the Witwatersrand, Johannesburg, 1 Jan Smutslaan, Braamfontein 2050, ZA. email: craig.carlson@aalto.fi
Nicole Anderton, Department of Biomedical Technology, Faculty of Medicine and Health Technology, Tampere University, FI.
Vered Aharonson, School of Electrical and Information Engineering, University of the Witwatersrand, Johannesburg, Braamfontein, ZA and Medical School, University of Nicosia, CY.
Naoyuki Otake, Hu Xinyue, Momoka Yamasaku, Mamoru Hashimoto, Nobuki Kudo, Division of Bioengineering and Bioinformatics, Faculty of Information Science and Technology, Hokkaido University, JP.
Michiel Postema, Department of Biomedical Technology, Faculty of Medicine and Health Technology, Tampere University, FI and School of Electrical and Information Engineering, University of the Witwatersrand, Johannesburg, ZA.

1 Introduction

A bubble collapsing near an interface may result in the formation of a liquid jet protruding form the distal bubble side, through the bubble, towards the interface.The formation of liquid jets has been studied to understand erosion processes [1, 2]. Microscopic jetting phenomena have been under investigation for their potential medical applications as microscopic injection needles facilitation ultrasound-guided drug delivery [3, 4]. The production of shock waves associated with jetting [2, 5] has applications in lithotripsy [6]. However, jetting with the aid of ultrasound has only been observed at acoustic pressure amplitudes allowing for inertial cavitation to occur but that are considered unsafe in humans [7], because of free radical and heat production [8]. Yet, the presence of cavitation nuclei has been known to alter and typically slightly lower the inertial cavitation threshold [9]. In addition, the presence of other cavities has been demonstrated to facilitate jet formation between bubble pairs [10]. According to theory and numerical simulations, placing bubbles in a semiconfined or confined space, such as vasculature, drastically increases the occurrence of jetting [11]. Therefore, ultrasound-guided bubble-assisted drug or gene delivery might be feasible at acoustic amplitudes below the inertial cavitation threshold.

The purpose of this study was to investigate the feasibility of generating jetting in a fluid under acoustic conditions considered safe for diagnosis, by introducing an agent that has been observed to release gas contents [12] in a confined space.

Let us assume a microscopic spherical gas bubble in an infinite fluid. If the bubble is subjected to an ultrasound pulse, its radial response can be expressed by a Rayleigh-Plesset equation. A simplified equation for ultrasound-driven micro-

bubble pulsation has been derived in a prior publication [9]. Incorporating viscous, reradiation, and thermal damping terms yields [13]:

$$R\ddot{R}+\tfrac{3}{2}\dot{R}^2=\frac{1}{\rho}\left[\left(p_0-p_\mathrm{v}+\frac{2\sigma}{R_0}\right)\left(\frac{R_0}{R}\right)^{3\gamma}+p_\mathrm{v}-\frac{2\sigma}{R}-\delta\omega\rho R\dot{R}-p_0-p(t)\right], \tag{1}$$

where $p(t)$ is the time-dependent driving function, p_0 is the ambient pressure, p_v is the vapour pressure, R is the instantaneous bubble radius, R_0 is the initial bubble radius, γ is the ratio of specific heats, δ is the total damping coefficient, ρ is the liquid density, σ is the surface tension, and ω is the angular driving frequency. For a bubble without a shell, the damping coefficient consists of three components [14, 15],

$$\delta=\delta_\mathrm{v}+\delta_\mathrm{r}+\delta_\theta\ , \tag{2}$$

where

$$\delta_\mathrm{v}=\frac{4\eta}{\omega\rho R^2} \tag{3}$$

is the viscous damping [14], in which η is the dynamic viscosity of the surrounding medium,

$$\delta_\mathrm{r}=\frac{\omega R}{c} \tag{4}$$

is the damping owing to reradiation [14], in which c is the speed of sound, and

$$\delta_\theta=\frac{\frac{\sinh X+\sin X}{\cosh X-\cos X}-\frac{2}{X}}{\frac{X}{3(\gamma-1)}+\frac{\sinh X+\sin X}{\cosh X-\cos X}}\left(\frac{\omega_\mathrm{r}}{\omega}\right) \tag{5}$$

is the thermal damping, in which in which $X=\frac{R_0}{l_\mathrm{D}}>1$ and ω_r is the angular resonance frequency of the bubble. Here,

$$l_\mathrm{D}=\sqrt{\frac{K_\mathrm{g}}{2\,\omega\,\rho_\mathrm{g}C_\mathrm{p}}}\ , \tag{6}$$

where C_p is the specific heat of the gas, K_g is the thermal conductivity of the gas, l_D is the thermal layer boundary thickness, and ρ_g is the density of the gas [16]. The ratio of angular frequencies in (5) is often squared or ignored [13–16]. The asymmetric collapse of a bubble may lead to the formation of a liquid jet [7, 10].

2 Materials and methods

Solutions of (1) were computed using the ode45 differential equation solver of MATLAB® (The MathWorks, Inc., Natick, MA, USA), assuming the following parameters constant: $c=1480\,\mathrm{m\,s^{-1}}$, $C_\mathrm{p}=1000\,\mathrm{J\,kg^{-1}\,K^{-1}}$, $K_\mathrm{g}=0.025\,\mathrm{W\,m^{-1}\,K^{-1}}$, p_0=101 kPa, p_v=2.33 kPa, γ=1.4, $\eta=1.00\,\mathrm{mPa}$, $\rho=998\,\mathrm{kg\,m^{-3}}$, $\rho_\mathrm{g}=1.00\,\mathrm{kg\,m^{-3}}$, $\sigma=0.072\,\mathrm{N\,m^{-1}}$, and $\omega=2\pi\times1.0\times10^6\,\mathrm{s^{-1}}$.

The initial radius was chosen on the interval $R_0\in[0.1\ ,\ 10]\,\mu$m. The linear bubble resonance frequency was computed using [17]

$$\omega_\mathrm{r}=\ \frac{1}{R_0\sqrt{\rho}}\sqrt{3\gamma\left(p_0-p_\mathrm{v}+\frac{2\sigma}{R_0}\right)+\frac{2\sigma}{R_0}-\frac{4\eta^2}{R_0^2\rho}}\ . \tag{7}$$

Free-field hydrophone data were used as an input driving function. To account for the presence of the compartment, $p(t)$ was amplified by an empiric step function to match the simulated radial excursions to those observed.

A quantity of 5 mg freeze-dried Quantison™ ultrasound contrast agent (Upperton Limited, Nottingham, UK), comprising albumin-encapsulated air bubbles, was stirred through 5 ml of degassed distilled water (FUJIFILM Wako Pure Chemical Corporation, Chuo-ku, Osaka, Japan). The median bubble diameter was measured from optical microscopy to be $5.2\pm0.9\,\mu$m [12]. For each experiment, a 200-μl droplet of this reconstituted ultrasound contrast agent was pipetted into a cylindrical compartment of 8-mm diameter and 2-mm height before being closed with an 18×18-mm Thickness No. 1 Micro Cover Glass (Matsunami Glass Ind.,Ltd., Kishiwada-shi, Osaka, Japan) and sealed with No.600M cloth tape (Sekisui Chemical Co., Ltd., Kita-ku, Osaka, Japan) [18]. The compartment was part of a 244×145×76-mm^3 Perspex container that was filled with degassed water and placed on top of an Eclipse Ti inverted microscope (Nikon Corporation, Minato-ku, Tokyo, Japan) with an S Plan Fluor ELWD 40×/0.60 objective lens (Nikon). The microscope was coupled to an HPV-X2 high-speed camera (Shimadzu, Nakagyo-ku, Kyoto, Japan) that was set to record at a frame rate of ten million frames per second [19]. The optical field of view coincided with the acoustic focus of a custom-built 1-MHz single element transducer mounted in the water container [19]. The transducer was driven by 3-cycle pulses with a centre frequency of 1 MHz and signal amplitudes between 0.50 V and 5.0 V. The signal was generated by an AFG320 arbitrary function generator (Sony-Tektronix, Shinagawa-ku, Tokyo, Japan) and amplified by a UOD-WB-1000 broadband power amplifier (TOKIN Corporation, Shiroishi, Miyagi, Japan).

In total, 54 high-speed experiments were performed. Each video recorded comprised 256 frames. The video frames were imported into the MATLAB® (The MathWorks, Inc., Natick, MA, USA) programming environment for further processing.

3 Results and discussion

The jetting phenomenon was observed in all experiments where gas release was occurring. The signal amplitude for gas

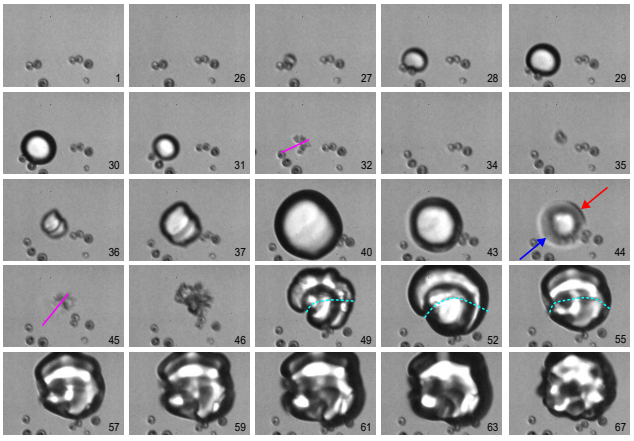

Fig. 1: Selected high-speed video frames, showing nucleation from Quantison™ (27), expansion to maximum (30), collapse (31) into a jet (32, —), explosive growth of coalescing fragments (35–37) to a maximum (40), collapse (43) generating a shock-wave (44) whose front (←) and wake (→) are indicated, collapse into a jet (45, —), expansion showing a needle jet (49–55, - - -), and surface harmonic oscillation (67). Frame numbers have been added to the lower right corners. Each frame corresponds to an area of $72 \times 48\,\mu\mathrm{m}^2$ and an exposure of $0.1\,\mu$s.

release was equal to or greater than 3 V for these events, which corresponded to a free-field mechanical index of 0.6.

In Figure 1, selected high-speed video frames are shown of Quantison™ microbubbles under sonication. A cavity was observed to have nucleated from a Quantison™ contrast microbubble in frame 27. This cavity was then seen to have expanded to a maximum size of $R = 11\,\mu$m in frame 30. Following collapse in frame 31, it was observed to undergo jetting in frame 32 over a distance of $17\,\mu$m. The resulting fragments were seen to have reappeared in frame 35. Coalescence was observed in subsequent frames until maximum expansion to $R = 21\,\mu$m of the remaining bubble in frame 40. The collapse of the bubble in frame 44 was interpreted to generate a shock-wave given the visible shock front and wake. This bubble collapse visibly resulted into a jet with a length of $26\,\mu$m in frame 45. During the subsequent expansion, a needle jet was visible in frame 55. The remaining bubble was observed to be non-spherical. It showed surface harmonic oscillations in frame 67.

Another example is shown in Figure 2. Here, a cavity was observed to have nucleated from a Quantison™ contrast microbubble in frame 27. This cavity was seen to have undergone expansion to a maximum of $R = 11\,\mu$m in frame 29, followed by collapse and translation. During the subsequent pulsation cycle, explosive growth was observed to a maximum expansion of $R = 16\,\mu$m in frame 39. The collapse of the bubble in frame 42 was interpreted to generate a shock-wave. This bubble collapse resulted into a jet as spanning a distance

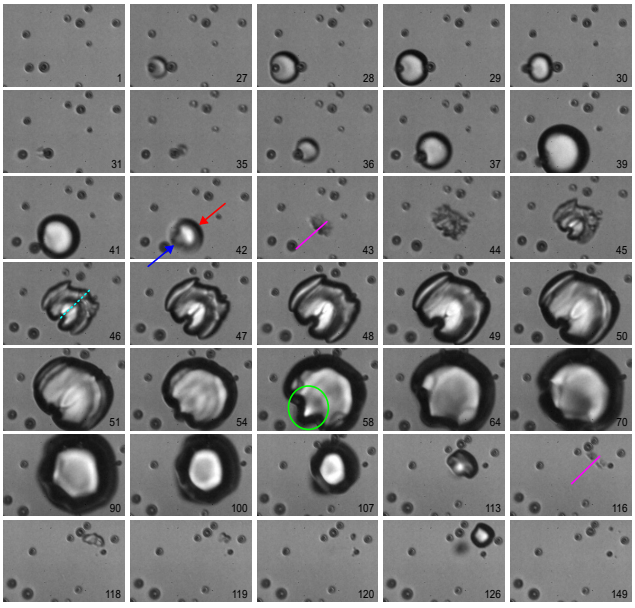

Fig. 2: Selected high-speed video frames, showing nucleation from Quantison™ (27), expansion to maximum (29), collapse and translation (30–35), explosive growth to a maximum (39), collapse (41) generating a shock-wave (42) whose front (←) and wake (→) are indicated, resulting into a jet (43, —), expansion showing a needle jet (46, - - -), formation of a reentrant jet (58, ○), asymmetric collapse (113), jetting (116, —), and radial pulsation (120–149). Frame numbers have been added to the lower right corners. Each frame corresponds to an area of $72 \times 48\,\mu\mathrm{m}^2$ and an exposure and interval of $0.1\,\mu$s.

of $27\,\mu$m. During the subsequent expansion, a needle jet was visible in frame 46. This needle jet was seen to break and result in a reentrant jet in the opposite direction of the original jetting direction in frame 58. Following asymmetric collapse in frame 112, a displacement was measured in frame 118, corresponding to a jet length of $26\,\mu$m. Its final equilibrium radius was measured to be $R = 1.4\,\mu$m in frame 149.

The jet lengths measured had been estimated from visible gas displacement between the bubble radius on the verge of collapse and the first visible appearance after jetting. Here, the verge of collapse was defined as first signs of asymmetry. It should be noted that the actual liquid jet displacement is approximately three times the bubble radius on the verge collapse [7], but that the visible displacement of the gas was consistently twice the radius upon collapse throughout our experiments.

Figure 3 shows two simulated $R(t)$ curves of a microbubble subjected to a 3-V pulse, one for which the presence of a confining space has been accounted for in the amplification function by multiplying the free-field pulse amplitude by a factor of six, and the other for which the presence of a confinement has been ignored. The measured excursions from two different events appear to match the former curve closer than the

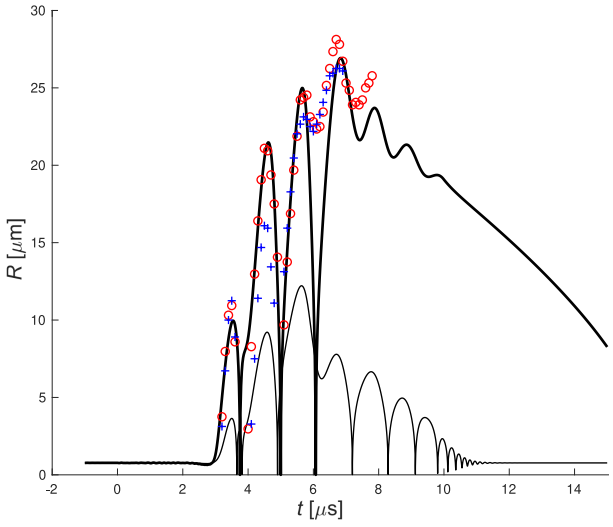

Fig. 3: Simulated $R(t)$ curves of a microbubble subjected to a 3-V pulse, accounting for the presence of a confining space (bold) and ignoring the presence of a confinement (thin), overlain by measured excursions from two different events (○,+).

latter. Despite the highly nonlinear and asymmetric behaviour of bubbles in a confined space, the Rayleigh-Plesset bubble model with additional damping terms and modified driving function well represented the spherically symmetric pulsation excursions experimentally observed.

4 Conclusions

In conclusion, jetting was observed to occur with microbubbles nucleated from ultrasound contrast agent microbubbles. Visible jet lengths of twice the bubble radius on the verge of collapse were measured. Owing to the confined space, the local acoustic amplitude was amplified to surpass the cavitation threshold. This finding is of interest for medical ultrasonic applications where the local environment comprises reflectors.

Author Statement

Research funding: This work was supported by JSPS KAKENHI, Grant Numbers JP17H00864 and JP20H04542, by the Academy of Finland, Grant Number 340026, and by the National Research Foundation of South Africa, Grant Number 127102. Conflict of interest: Authors state no conflict of interest. Informed consent: Authors state that informed consent is not applicable. Ethical approval: Authors state that no ethical approval was required for this research as no human or animal samples or data were used. This manuscript was written according to recipe [20], without the aid of artificial intelligence.

References

[1] Reuter F, Mettin R. Electrochemical wall shear rate microscopy of collapsing bubbles. Phys Rev Fluids 2018;3:063601.
[2] Reuter F, Deiter C, Ohl C-D. Cavitation erosion by shock-wave self-focusing of a single bubble. Ultrason Sonochem 2022;90:106131.
[3] Prentice P, Cuschieri A, Dholakia K, Prausnitz M, Campbell P. Membrane disruption by optically controlled microbubble cavitation. Nature Phys 2005;1:107–10.
[4] Postema M, van Wamel A, ten Cate FJ, de Jong N. High-speed photography during ultrasound illustrates potential therapeutic applications of microbubbles. Med Phys 2005;32:3707–11.
[5] Reuter F, Ohl C-D. Supersonic needle-jet generation with single cavitation bubbles. Appl Phys Lett 2021;118:134103.
[6] Eisenmenger W. The mechanisms of stone fragmentation in ESWL. Ultrasound Med Biol 2001;27:683–93.
[7] Ohl C-D, Ikink R. Shock-wave-induced jetting of micron-size bubbles. Phys Rev Lett 2003;90:214502.
[8] Aikawa T, Kudo N. Relation between thresholds of free radical generation and atomization under ultrasound exposure. Jpn J Appl Phys 2021;60:SDDD13.
[9] Carlson CS, Matsumoto R, Fushino K, Shinzato M, Kudo N, Postema M. Nucleation threshold of carbon black ultrasound contrast agent. Jpn J Appl Phys 2021;60:SDDA06.
[10] Biller B, Hoppe N, Adami S, Adams NA. Jetting mechanisms in bubble-pair interactions. Phys Fluids 2022;34:076111.
[11] Krasovitski B, Kimmel E. Gas bubble pulsation in a semi-confined space subjected to ultrasound. J Acoust Soc Am 2001;109:891–8.
[12] Anderton N, Carlson CS, Poortinga AT, Xinyue H, Kudo N, Postema M. Sonic cracking at low acoustic amplitudes. Proc UltraSonic Electronics Symp 2023;44:2E1-3.
[13] Anderton N, Carlson CS, Aharonson V, Postema M. Determining the influence of endoskeleton friction on the damping of pulsating antibubbles. Curr Dir Biomed Eng 2022;8:781–4.
[14] Devin C. Survey of thermal, radiation, and viscous damping of pulsating air bubbles in water. J Acoust Soc Am 1959;31:1654–67.
[15] Medwin H. Counting bubbles acoustically: a review. Ultrasonics 1977;15:7–13.
[16] Eller AI. Damping constants of pulsating bubbles. J Acoust Soc Am 1970;47:1469–70.
[17] Kudo N, Uzbekov R, Matsumoto R, Shimizu R-i, Carlson CS, Anderton N, et al. Asymmetric oscillations of endoskeletal antibubbles. Jpn J Appl Phys 2020;59:SKKE02.
[18] Poortinga AT, Postema M, Carlson CS, Anderton N, Yamasaku M, Otake N, et al. Sonic cracking of calcium carbonate-encapsulated microbubbles observed at moderate acoustic amplitudes. Curr Dir Biomed Eng 2023;9:37–40.
[19] Kudo N. High-speed *in situ* observation system for sonoporation of cells with size- and position-controlled microbubbles. IEEE Trans Ultrason Ferroelectr Freq Control 2017;64:273–280.
[20] Carlson CS, Postema M. A pocket-sized recipe for cooking up a scientific manuscript. Tampere: Tampere University 2023.